International Journal of Advanced Technology and Engineering Exploration, Vol 9(95)
ISSN (Print): 2394-5443 ISSN (Online): 2394-7454
http://dx.doi.org/10.19101/IJATEE.2021.875874

Research Article

Average torque improvement of BLDC motor in battery electric vehicle

Rupam[1*], Sanjay Marwaha[2] and Anupma Marwaha[3]
Research Scholar, Department of Electrical and Instrumentation Engineering, Sant Longowal Institute of Engineering and Technology, Sangrur, Punjab, India[1]
Professor, Department of Electrical and Instrumentation Engineering, Sant Longowal Institute of Engineering and Technology, Sangrur, Punjab, India[2]
Professor, Department of Electronics and Communication Engineering, Sant Longowal Institute of Engineering and Technology, Sangrur, Punjab, India[3]

Received: 27-April-2022; Revised: 12-October-2022; Accepted: 14-October-2022

Abstract
Amongst automobiles, the domain of electric vehicles is being targeted globally by researchers from its inception. Hence, a great proliferation in the advancement of electric vehicles has been documented in recent years. The cogging torque of the motor is the main cause of acoustic noise and vibration produced in the electric vehicle. The objective of this paper is to minimize the cogging torque and improve the average torque of the brushless direct current (BLDC) motor used in battery electric vehicles. The power rating of the selected reference vehicle is computed using kinematic equations. The selection of material and pole slot combination has a great impact on motor torque which influences the overall performance of the vehicle. An optimal design of a BLDC motor is presented by selecting distinct values of rotor pole embrace factor by using a parametric approach of ANSYS Maxwell software. With the help of the finite element method (FEM), the magnetic analysis of the proposed motor has been carried out. Consequently, it is observed that the designed model offers significant reduction in cogging torque with improved average torque of the motor. Accordingly, the rating of the battery to power the motor for propulsion has been computed.

Keywords
Battery electric vehicle, BLDC motor, Finite element analysis, Permanent magnet.

1.Introduction
Over the last number of years, global warming has been a significant concern around the world. The unpredictable climatic fluctuations have been observed due to this reason in all areas of the planet. Conventional transportation using fossil fuels is one of the major sources of global warming. To minimize climate change, developed nations are making a sustainable effort to reduce carbon dioxide (CO_2) and other greenhouse gas (GHG) emissions [1, 2]. One of the most important technologies for reducing (GHG) emissions is the electrical mobility of transportation systems. Poor air quality has shifted interests from the scientific community to electric vehicle (EV), which can potentially reduce fuel costs and overpower the current energy crisis. Some developed nations have set a target of having zero emission vehicles (ZEVs) on the road by 2050 [3, 4].

Due to rising prices for conventional fuel and environmental concerns the government of India is also paying greater attention to EV. The electric mobility regulations allow the government to provide subsidies with less paperwork. In the starting phase, two and three-wheelers (2W and 3W) vehicles has been considered as the backbone of electrification since they have a significant market share for transportation in rural areas [4, 5].

Among the various components of the battery electric vehicle (BEV) architecture, electric motors play a significant part. The electric motor anticipated low torque ripple, great power density, a wide-speed range, and high efficiency [6, 7]. In the EV industry, conventional motors such as the switched reluctance motor (SRM), permanent magnet synchronous motor (PMSM), induction motor (IM), and direct current (DC) motor were in use. Induction motors have smaller market share in automobile industry despite of having higher durability and robustness [8, 9]. Further induction motors are well known for

*Author for correspondence

maintenance free operation, low cost and greater overload capacity as compared to other motors. Conventional motors can also work well with current drive designs, but with their inefficiency in lower speed ranges, they are less effective due to high losses and limited constant power range. In EV, however, conventional control approaches are unable to provide performance requirements. The SRM motor has some advantages, but the major challenges for EV are noise and torque ripples [8−11]. Although PMSM motors are also very efficient, have a high-power density, and require a control strategy, but the drive controller is very expensive in comparison to other motors [12, 13].

Permanent magnet brushless direct current (PMBLDC) motors have found increased popularity due to their efficiency and versatility [14]. Among commutator-less machines, Brushless direct current (BLDC) motor has received overwhelmingly positive appraisal in the literature. This motor operates at moderate speeds but has several desirable characteristics, including a simple design, sufficient mechanical features, excellent efficiency, a light weight, low rotary inertia, and precise control [15−18]. However, some of the drawbacks are demagnetization and cogging torque [18]. The power density is a vital factor for the motor, the higher is the power density the lower is the fuel consumption of the vehicle [19].

This paper examines the BLDC motor's parameter estimation with a focus on lowering cogging torque and refinement of average torque of the motor used in BEV. According to the power rating of the motor the battery sizing has been calculated. To improve the performance of the model, parametric analysis method is used. Using computational electromagnetic tool ANSYS Maxwell, the BLDC model has been simulated, while considering pole embrace factor as design variable. The final model reduces torque ripple while improving average torque. If no changes observed in the motor's performance, the design variable is updated with the finite element adaptive technique. The simulation results and comparisons between the base design [20] and proposed motor design is discussed later in the manuscript.

This paper has been organized in different sections: Section 2: Focus on the literature review of the BLDC motor. Section 3: Deals with the parameter matching of the vehicle with the selection of permanent magnet material. Further it illustrates the designed model of motor.

Section 4 and 5: Emphasizes on the simulated results and highlights the limitations of present work. Section 6: Shows the conclusion related to the design of the motor.

2.Literature review

Researchers have always shown their interest in the mathematical modelling and design of EV and are concerned about application aspects of the various computational electromagnetics techniques for performance enhancement of motors used in these vehicles. Toker et al. [19] studied axial flux type and hub motor for the light electric vehicle with genetic algorithm (GA) and experimental results and as claimed efficiency of the motors significantly improved. However, the authors in this paper have not discussed the adaptiveness of finite element models.

Thenmozhi et al. [21] discussed the BLDC motor for EV considering Alnico magnet suitable for lowering the cogging torque of the motor. However, Neodymium based magnets are used for BLDC and PMSM. Challenges and limitations of Alnico based magnets have not been highlighted in the paper. Guo and Wang [22] presented the design of a permanent magnet motor of the surface-mounted type by using finite element method (FEM) to choose the ideal combination of the pole arc coefficient, rotor pole, and stator slot. The advantage of this method is that the electromagnetic ripple gets weakened and stability is achieved. Limitation of work is that an appropriate stator slot and rotor pole combination can only guarantee the operational stability of the motor. Vadde and Sachin [23] presented the design of a surface-mounted BLDC motor with three alternative stator and rotor configurations for two-wheeler EV. The generalized design of the paper has been focused only on three parameters i.e., torque, speed and efficiency have ignored other crucial vehicle parameters. Minh et al. [24] presented paper on BLDC motor design with several permanent magnet configurations on the rotor for use in EV. Authors have discussed skewing of the rotor slots and have used various permanent magnet shapes to reduce the torque ripple of the motor. However, in this paper the authors have not used a single platform for design and analysis of the problem which results in uncertainty of the designed model.

Khalid et al. [25] developed a better optimum FEM design of BLDC for the application of bicycles. The model achieved better torque, by increasing the consumption of permanent magnet that however

enhanced the cost of the motor. Kumar et al. [26] proposed the motor design of BLDC in a manuscript with the different slot types having the same slot area. This paper does not take into consideration the crucial factor of speed for analysis point of view. Du et al. [27] proposed the design of motors for high-speed applications. Best part of the paper is that it deals with multi physics constraints of the model. However, the magnetic field analysis of the paper has been side-lined, which plays a vital role in deciding the rotor stability due to magnetic forces acting on the motor under running conditions. Li et al. [28] discussed the design of the permanent magnet flux switching machine for propulsion of EV. Performance was analysed using current vector strategy. The limitation of the paper is that even under the under rated conditions, the efficiency of the motor is only 85%. Sandeep and Shastri [9] illustrated motor design using computer aided finite element analysis (FEA) tool for application of three-wheeler vehicle. Paper does not cover the self-adaptive FEA, so has limitations of customized design. Yuan et al. [29] design of BLDC where pole arc coefficient and air gap length were optimized for medium speed EV. However, in this model only two parameters i.e., pole arc coefficient and air gap length have been considered to find an optimized model.

He and Wu [30] proposed the design of motor and generator based on the three design variables. Since the authors mainly focused on Multiphysics problem with focus on thermal analysis and less emphasis has been laid on the electrical performance parameters. Mithunraj et al. [31] proposed design of BLDC motor with the help of RMxprt, and then transient analysis had been carried out based on Maxwell 2D design. Limitation of the work is that authors have skipped finite element adaptivity concept. Leitner et al. [32] had discussed the design of a claw-shaped sub fractional-based BDLC motor. Punching arrangement and claw skewing are used to test the motor's performance and demonstrate the technique for minimising cogging torque. Authors have reduced torque ripples at low speed of motor but have not commented about torque ripple reduction at medium and high speeds. Popescu et al. [33] proposed some changes in the prior winding of electric motors which enhanced the performance of the motor depending on the material used. Generalized solutions of traction systems for light motor vehicles (LMV) have been discussed in paper but no in-depth analysis has been carried out. Patel and Suthar [34] provided the optimal design of the Axial flux surface-mounted permanent magnet type brushless DC motor (AFSPMBLDC) with the use of a GA. The motor model depends on improved design variables, and the goal of this analysis was to present the best possible combination of design factors that could be gained by using the GA as an optimization technique. Final validation was performed using 3D FEA. However, this type of optimization cannot be generalized and usually not effective with high rating power motors.
Yildirim et al. [35] proposed the design of BLDC motor using permanent magnets. Four different types of magnets were used to analyse the motor's performance, after which the geometry-based values for back electro-motive force (EMF), magnetic flux density, and cogging torque were upgraded. In this paper the authors have not considered the refinement strategies of the mesh i.e., the degree of freedom has not been varied. He and Wu [36] proposed FEM based design of internal permanent magnet brushless DC motor (IPMBLDCM) for the electrical tools like wrench system. An improved equivalent magnetic circuit was created to verify working temperature and flux leakage for the initial design. However, being the Multiphysics problem having temperature as one of the crucial parameters, authors have not deeply analysed the electromagnetic design of the BLDC motor. Saed and Mirsalim [37] designed a dual stator permanent magnet type BLDC motor. The simulation results of Maxwell and MATLAB were compared with the effect of mutual inductance and state space equations. In this paper the authors have not analysed the delaunay triangulation mesh and not opted the refinement strategies for improvement of results.

As per the literature survey it has been observed that the authors have mainly concentrated their efforts to analyse the electrical and magnetic field parameters especially efficiency, torque, and speed of the BLDC motor with different techniques. Some of the researchers have attempted the Multiphysics domain considering temperature as one of the prime factors. However, it has been observed that the implementation of the finite element tool has not been implemented judicially to compute vital parameters of the motor in holistic way. Finite element refinement strategies have not been used in these papers. In this paper attempt has been made to address the limitation of earlier work and average torque of BLDC motor used in BEV has been improved with h-adaptivity FEA. Battery size to propel such motor has been matched accordingly.

3.Methods

There are numerous ways to design the motor for the respective applications. The most important parameters that are usually considered for motor design are material selection and dimensional variations. The growing use of high-performance processing systems is energising the development of computational electromagnetics and improving the numerical tools to analyse such field problems. These electromagnetic explorations by use of fast processors saves time and money [38]. To solve the behaviour equations of electrical machines, numerical methods are being used. For the analysis of electromagnetic devices, the FEM is one of the most reliable, flexible, and worthwhile. This method is used to perform an electromagnetic analysis of electrical machines, enabling the determination of flux leakage distributions in a steady state at the areas of concern, which allows for flux and flux density determination [39−42]. The reason for this is that complex geometries can be easily modelled and analysed by FEM. This technique can be used to determine electromagnetic field distribution and integral parameters in the design of rotating machines without any significant knowledge of applied mathematics. A substantial amount of research has been conducted on the design of motors using FEM [43−45].

The flow sequence regarding implementation of the adaptive finite element technique is shown in *Figure 1*. FEA consists of primarily three stages. The pre-processing is the very first stage in which the geometrical domain and simplifications in the form of variable is done. The discretization of the model into finite nodes and their corresponding nodal equations are formulated. The second stage is processing, in which the actual solution or analysis part is dealt. The configuration of type of analysis required based on loading conditions (static or dynamic loads) and material details such as model analysis, static analysis, linear or non-linear analysis is considered, under this phase [44, 45]. The last stage is post-processing, in which software contains classy routines used for sorting, printing, plotting, and comparing results obtained at the processing stage with analytical results. Refinement strategies such as h-type, p-type and hp type are considered in this stage. After this, junction error analysis is done. Then, results get displayed in graph, tabular or visual form [45].

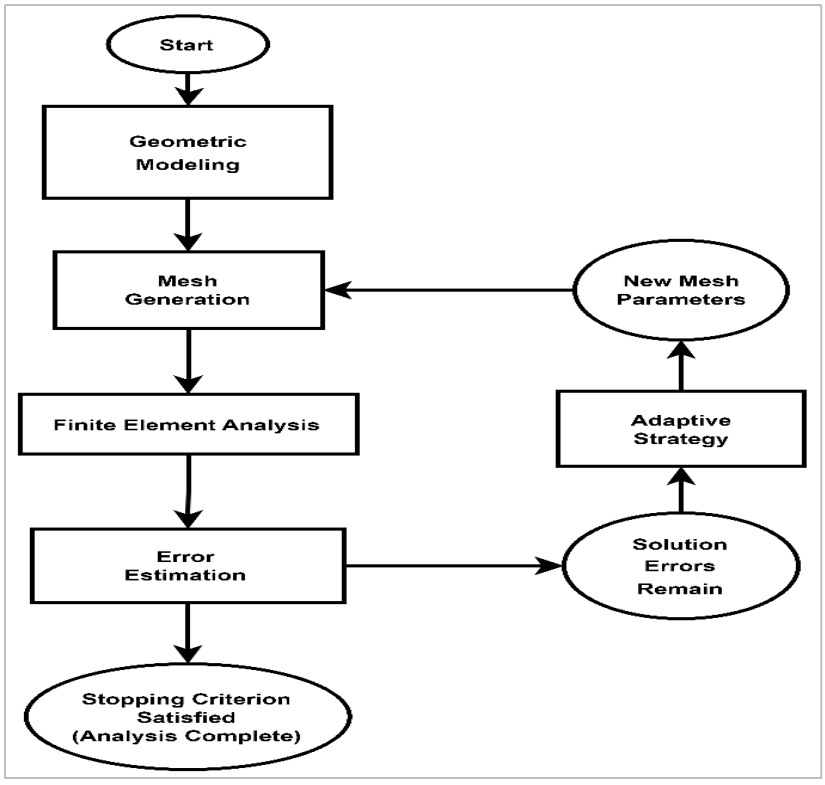

Figure 1 Flow sequence of adaptive solution algorithm

Figure 2 shows the block diagram of the system using BLDC motor drive for BEV. To compute the crucial motor parameters, this system is combined with the finite element setup. The three primary system units that make up a BEV operation are the motoring unit, the battery management unit, and the power electronic controlling unit (consists of controller and converter). The motor and other components required for the vehicle's effective functioning are powered by the battery pack, which is the heart of the BEV model. The power converter converts energy to optimum level from battery as required by the motor. The bi-directional converter helps in delivering regenerative energy to the battery, providing charging when the vehicle decelerates. The vehicle frame is represented by the set of wheels that are attached to the motor by a transmission system. With the aid of the controller, which analyses load requirements and generates proportional control signals with the assistance of feedback from the vehicle to achieve a smooth and efficient functioning of the vehicle, the motor draws power from the battery in accordance with the demands of the load. Drive cycle source is an example of driving pattern used in the simulation according to the drive cycle data. The rated power rating of motor has been kept according to the selected reference vehicle [46, 47]. The model of BLDC motor has been designed using licensed ANSYS Maxwell software package. The controlling unit consists of a position sensor for sensing the exact rotor position. Phase convertor is a unit which converts the input DC voltage into commutated phase voltages to energize the BLDC phase windings. Since, 24/18 pole/slot combination of BLDC motor is a three-phase machine, the phase convertor converts the input voltage into three phase commutated voltage and is basically a three- phase inverter. For EV all the speed ranges need to be considered for efficient controlling, and hence the position of rotor plays a vital role in rotating the motor. Hence hall sensor commutation in BLDC provides better performance for EV applications. Different standard control strategies could be used for BLDC motor drive system. Commutation control with hall sensor and speed control can be done with varying DC input voltage [48, 49].

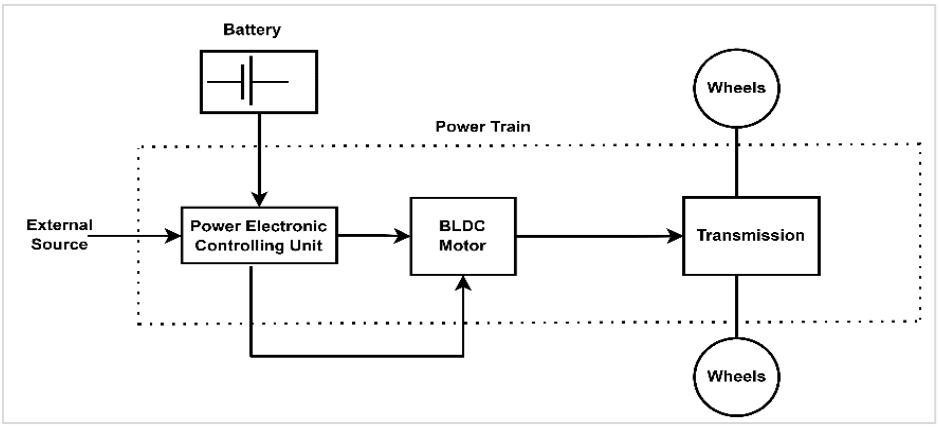

Figure 2 Block diagram of battery electric vehicle system

The parameter matching of the motor with the EV is necessary before developing the motor and is covered in this section. Later in the section, the required material selection and mathematical modelling of the motor are also discussed.

3.1Kinematic dynamic equation of BEV

The performance of the BEV with the BLDC motor is taken into consideration while formulating the dynamic equations. With the use of initially presumptive parameters, the driving resistive forces of the vehicle can be calculated using the EV characteristics. The torque and power needs for driving conditions have been determined using vehicle dynamic equations [50, 51]. Schematic presentation shown in *Figure 3* depicts the force acting on the vehicle.

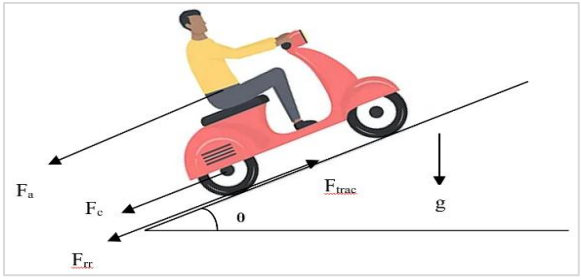

Figure 3 Tractive force representation on a vehicle

There has been a brief discussion of the equations for the tractive power and torque in addition to the different types of forces acting on the vehicle. The aerodynamic drag force (Fa) in Equation 1 is because of the friction of the vehicle moving through air. The coefficient of drag is Cd, velocity of the vehicle is v, and rho (ρ) is the air density at sea level. This force is directly square of the velocity, frontal area of vehicle, body shape.

$$F_a = \frac{1}{2}\rho\, A\, C_d v^2 \quad (1)$$

The rolling resistance force (F_{rr}) in Equation 2 is dependent on the selection of the tire. The coefficient of rolling resistance is u_{rr}, gravitational force is g, and gradient angle is Θ. This force is directly proportional to the coefficient of rolling coefficient.

$$F_{rr} = m\, g\, \mu_{rr}\, Cos\Theta \quad (2)$$

The climbing force (F_c) in Equation 3 is needed to propel the vehicle up a slope where vehicle gross weight is m.

$$F_c = m\, g\, Sin\Theta \quad (3)$$

The total tractive force (F_{trac}) in Equation 4 is the combination of all the resistive forces need to overcome the friction.

$$F_{trac} = F_a + F_{rr} + F_c \quad (4)$$

The tractive power can be calculated and represented as (P_{trac}). It can be written as in Equation 5.

$$P_{trac} = F_{trac}\, v \quad (5)$$

The tractive torque (T_{trac}) on the vehicle wheel is calculated by the force in Equation 6.

$$T_{trac} = F_{trac} * r_{wheel} \quad (6)$$

As indicated in *Table 1*, the reference vehicle chosen is a two-wheeler with values for the parameters total weight, air drag coefficient, rolling coefficient, etc.

Table 1 Initial selected parameters of BEV

Parameter	Value
Total Weight (m)	250 Kg
Specific Acceleration (g)	9.81 m/s^2
Coefficient Rolling resistance (μ_{rr})	$4*10^{-2}$
Wheel Diameter of Vehicle (d)	0.432 m
Density of Air (ρ)	1.23 Kg/m^3
Drag Coefficient (C_d)	0.88

The BEV should be able to perform a complete trip using energy stored in the battery pack without violating the primary constraints of the battery pack. For this a standard speed profile was selected i.e. Indian driving cycle (IDC) considering flat road. The velocity versus time variation of IDC for testing of this vehicle is shown in *Figure 4*. This test is of 111 second duration having typical drive profile with a maximum speed of 50 kmph. The battery pack voltage is vital as the type of the associated electronic power control (EPC) unit depends on it. The Lithium-Ion (Li-ion) battery used has approximately 15.2 Ah rating of the battery [12, 47]. The battery power rating can be calculated as the ratio of motor power to transmission efficiency (value of transmission efficiency can be 80-85%).

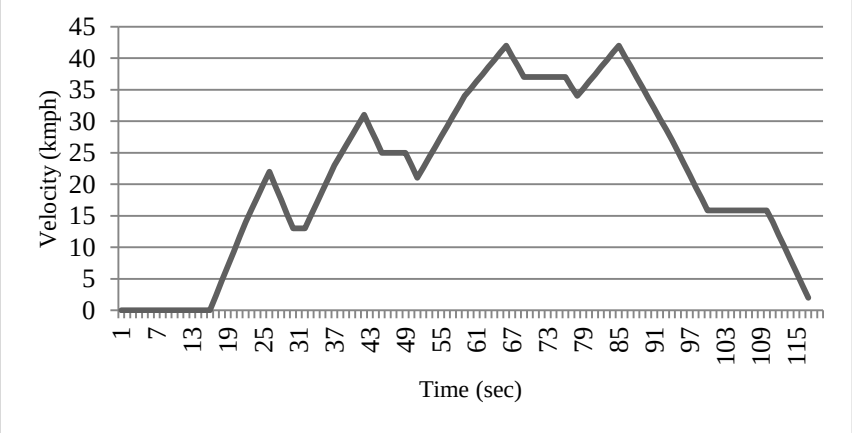

Figure 4 Velocity vs time graph of two-wheeler IDC

3.2Material of permanent magnet and pole/slot configurations

An appropriate selection of materials of the permanent magnet will allow the designer to overcome the limits of the demagnetizing effect and torque ripple at some reason. The presence of demagnetization cause heating and cogging torque is unfavorable because it makes noise and disturbing the eccentricity of rotor with backlash problem in bearings. ceramics (ferrites), alnicos (aluminum, nickel, cobalt, and iron), and rare earth magnet (samarium-cobalt, neodymium iron and boron) are the three types of permanent magnets used in electric motors. Due to high magnetic field density and low

magnetic field residual density at working and curie temperatures, the rare earth magnet neodymium iron and boron (NdFeB) is in high demand. Ceramic magnet materials are abundant and inexpensive, but their low retentivity results in a weak magnetic field. Samarium cobalt (SmCo) is the second strongest magnet material after NdFeB, although it is also the most expensive due to its narrower curie working temperature range [52−54]. Alnicos have low coercive forces so gets demagnetized easily. The recent development in rare-earth permanent magnet materials have opened new possibilities for BLDC motor design and application [52−56]. In *Table 2* information about the properties of the permanent magnet material found.

Table 2 Permanent magnet material properties

Properties	**Alnicos**	**Ceramic**	**SmCo**	**NdFeB**
Residual Density, B_r (T)	0.7-1.28	0.23-0.41	0.83-1.16	1.00-1.41
Coercive Force, H_c (kA/m)	37-143	50-290	480-840	760-1030
Max. energy product, BH_{max} (kJ/m^3)	10.7-71.6	8.35-31.8	130-240	220-366
Density, (g/cm^3)	6.8-7.3	4.9	8.4	7.4
Max. service temp, T_{max} (°C)	450-550	800	300-350	150

Selection of magnet materials is purely based on the type of application. The increased magnet thickness prevents demagnetization, while a greater airgap lowers noise levels and windage loss [53, 56]. *Figure 5* depicts the B-H curve representation of a permanent magnet's characteristics [52].

The magnitude and frequency of the cogging torque also affects with the selection of pole/slot combination. In fractional-slot motors fractional slot motors have reduced cogging torque with ratio value less than unity. A 24/18 (slots/pole) combination is selected for design. This provides slots/pole/phase value, which is less than 0.5 [20].

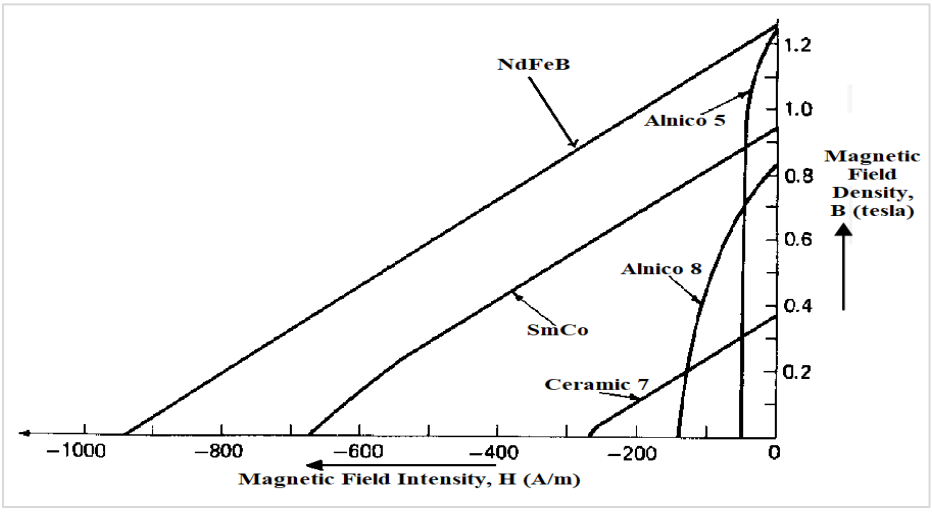

Figure 5 Permanent magnet material BH curve

3.3Mathematical equations of BLDC motor

The sizing for electrical machine design is given by Equation 7.

$$S = 11.k_{w1}.B.ac.\left(\frac{D}{100}^2\right).\frac{L}{1000}.n \quad (7)$$

where S is motor power, k_{w1} is winding factor, B is magnetic specific loading, electrical specific loading is ac, L is stack length, D is stator diameter, n is rated speed of the motor. The modelling of BLDC motor is proposed keeping in a view that undesirable cogging torque, leads to inefficient operation. In the BLDC motor, the cogging torque affects averaged torque thus generates undesired torque ripple. The cogging torque as stated in Equation 8 must be lowered to reduce noise and vibration [57].

$$T_{cog} = \frac{1}{2}\emptyset_g^2\frac{dR}{d\theta} \quad (8)$$

where flux of air gap is $\emptyset_g$ and air gap reluctance w.r.t. rotor angle dependent is $\frac{dR}{d\theta}$. The cogging torque will be reduced by reducing $\frac{dR}{d\theta}$ as they are directly

proportional to each other. The computation of the cogging torque is based on changing one mechanical degree angular rotation. It's worth noting that most cogging torque-reduction solutions also diminish the effective back EMF, resulting in generation of mutual torque. The voltage equation of three-phase BLDC equivalent circuit in matrix form is as shown in Equation 9.

$$\begin{cases} V_a=i_aR+L\frac{di_a(t)}{dt}+e_a \\ V_b=i_bR+L\frac{di_b(t)}{dt}+e_b \\ V_c=i_aR+L\frac{di_c(t)}{dt}+e_c \end{cases} \quad (9)$$

In compact form the equation can be expressed in Equation 10.

$$\hat{V} = f\left[\hat{I}, \Delta\hat{I}\right] \quad (10)$$

The back-EMF values are affected with number of rotations, rotor speed and with the magnetic field intensity. There is phase difference of 120° between each phase of three phase system. If back-EMF constant is λ, then back-EMF for each phases value is described as in Equation 11.

$$\begin{aligned} e_a &= \omega\,\lambda\,(\theta) \\ e_b &= \omega\,\lambda\,(\theta-\tfrac{2\pi}{3}) \\ e_c &= \omega\,\lambda\,(\theta+\tfrac{2\pi}{3}) \end{aligned} \quad (11)$$

Accordingly, back-EMF and phase current multiplication; taking into account all losses are the instantaneous power supplied. The input and output power of motor can be expressed as in Equation 12 and Equation 13.

$$P_i = i_a e_b + i_b e_b + i_c e_c \quad (12)$$

$$P_o = P_i - (P_{fw} + P_{cua} + P_t + P_{fe}) \quad (13)$$

where P_i is input power, P_{fe}, P_t, P_{cua}, and P_{fw} are iron, transistor/diode, stator copper losses; and windage and frictional losses. The expression of efficiency is stated in Equation 14, and it is computed by factoring output and input power along with losses.

$$\eta = \frac{P_o}{P_o+P_{fw}+P_{cua}+P_t+P_{fe}} \quad (14)$$

By ignoring, mechanical and stray losses, electromagnetic torque, T_e is obtained as shown in Equation 15 and Equation 16. The torque at any instant of rotor T(θ)is the arithmetic sum of averaged torque and torque ripple is represented in Equation 17. The average torque and torque ripple of the motor can be stated as Equation 18 and Equation 19.

$$T_e=(e_Ai_A+e_Bi_B+e_Ci_C)/\omega \quad (15)$$

$$T_e=P_i/\omega \quad (16)$$

$$T(\theta) = T_{avg} + T_{ripple} \quad (17)$$

$$T_{avg} = \frac{1}{\theta_1'-\theta_1}\int_{\theta_1}^{\theta_1'} T(\theta) \quad (18)$$

$$T_{ripple} = \frac{T_{max}-T_{min}}{T_{avg}} \quad (19)$$

where ω represents mechanical rotation/speed in rad/s, (θ_1' - θ_1) represents the complete electrical cycle, of the BLDC motor. The cogging torque can be minimized by selecting best value of embrace factor of rotor pole. Ratio of rotor pole pitch (β) pole arc (γ) in permanent magnet motor is defined as the rotor pole embrace factor as shown in *Figure 6.* Generally, its value is less than unity [58].

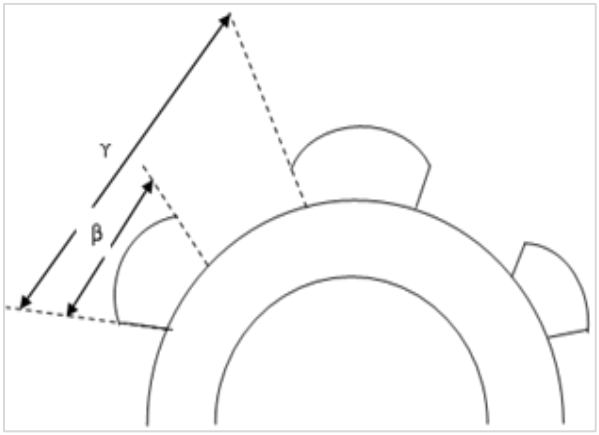

Figure 6 Rotor pole embrace factor diagram

3.4Design of BLDC motor

The ANSYS Maxwell software is being used to design outer rotor BLDC motor. The motor's dimensional specification is tabulated in *Table 3.* For designing of motor, rotor pole embrace factor is selected as the variable. The control type can be DC or current chopped control (CCC), for the model DC control type used.

Table 3 Dimensional specifications of BLDC motor

Parameter	Value
No of pole/slot	24/18
Stator outer diameter (D_{so})	180 mm
Stator inner diameter (D_{si})	90 mm
Stack length (L)	50 mm
Rotor outer diameter (Dr_o)	35.5 mm
Rotor inner diameter (Dr_i)	182 mm

The rated power and values of some constants of the BLDC motor is shown in *Table 4.*

Table 4 Rated constants parameters of BLDC motor

Parameter	Value
Rated Power	3.5 kW
Phase Inductance	0.00011 H

Phase Resistance	0.0793 Ω
Rated Torque Constant	0.577 (Nm/A)
Rated Speed	2000 rpm

Copper is the material used for the winding, and M27_26G silicone steel is the material used for the stator and rotor core. The BH curve of steel material is displayed in *Figure 7*.

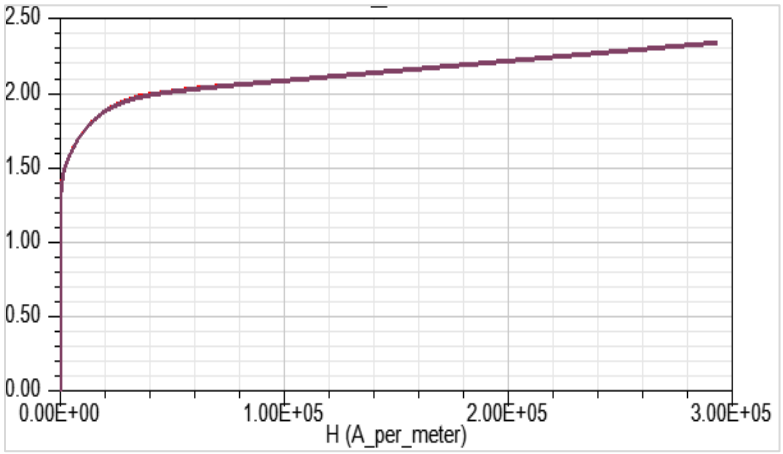

Figure 7 BH curve of M27_26G silicone steel sheet

4.Results

In this section the performance parameters of BLDC motor obtained after using ANSYS Maxwell software have been discussed and analysed at rated speed conditions. The achieved electrical and magnetic parameter results of the motor have been discussed.

4.1Parameter analysis of BLDC motor

The motor performance can be analysed from a variety of perspectives. For the smooth operation of the two-wheeler BEV the cogging torque and ripples of the motor must be decreased. The efficiency is one of the most important characteristics for the design of proposed motor. The rotor pole embrace factor variable has a considerable influence on the efficiency and cogging torque of the motor. The parametric method is applied to choose the selection of the pole embrace factor in the design. In the parametric process of optimizing the pole embrace values of rotor, the region should be taken into consideration where efficiency is maximum and cogging torque is minimum. Sometimes, it is not necessary to achieve highest value of efficiency and lowest value of cogging torque at same value of variable. For the optimum selection, value between different regions need to be selected. To achieve the optimum values of performance keeping in consideration the size of motor, the pole embrace factor referred as 'p' is varied from 0.4 to 0.6, considering it as a lower limit and upper limit having 0.02 step size. The cogging torque, rated torque, and efficiency with the change in rotor pole embrace factor value are obtained by parametric approach as shown in *Figure 8* and *Figure 9* respectively. At value 0.5, the cogging torque is least, and its value is 0.0353% of rated torque. Cogging torque is highest at 0.4 and its value is 28.27% of rated torque and at 0.52 its value is 6.1% of rated torque. The graph depicts that cogging torque is lowest at point 0.5 and at same point efficiency of motor is approximately 92.1%. The graphical representation also shows the lowest and intermediate values of the cogging torque and efficiency. The 92.37% efficiency is highest at pole embrace factor of 0.4 and is lowest of 91.81% at value 0.6.

The variation of cogging torque in respect to position of rotor is shown in *Figure 10*. As shown in the graph 0.005 Nm is the smaller value of cogging torque at point 0.5 and cogging torque of value 3.967 nm is the highest at point 0.4. The smaller value of cogging torque indicates less speed fluctuations, and better running stability.

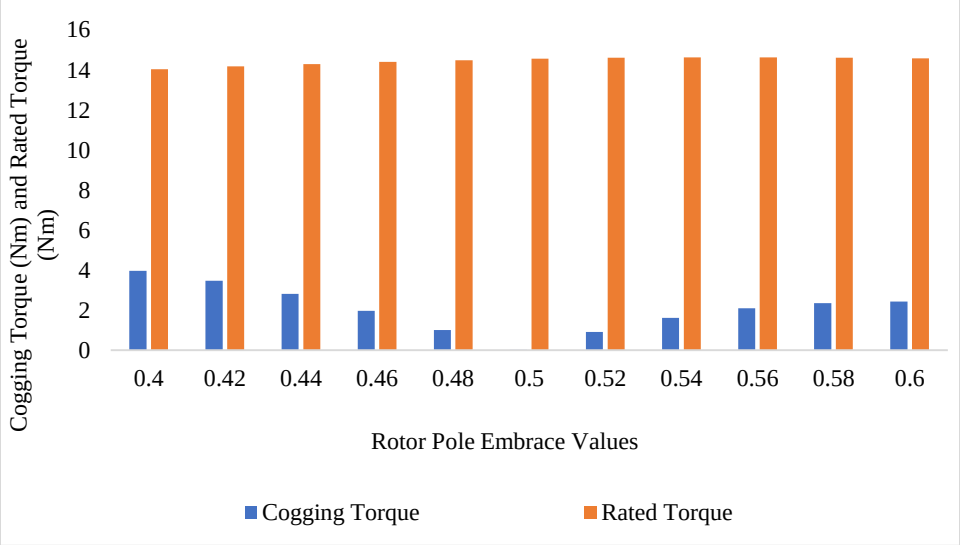

Figure 8 Graphical representation of cogging torque and rated torque with variation in rotor pole embrace values

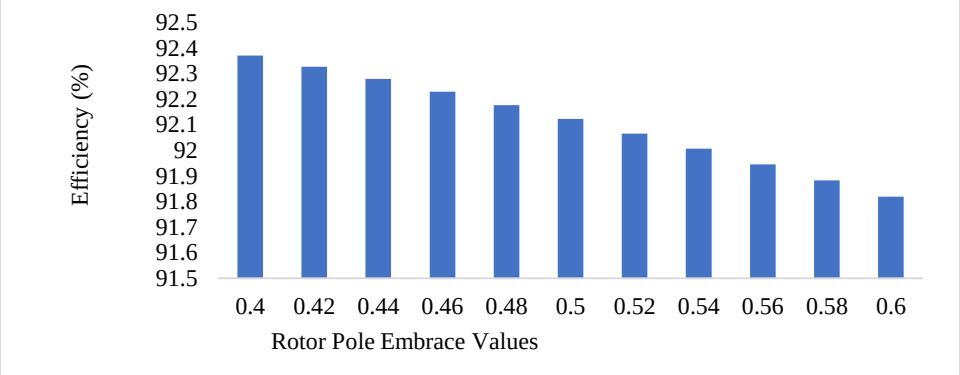

Figure 9 Graphical representation of efficiency in reference to rotor pole embrace factor

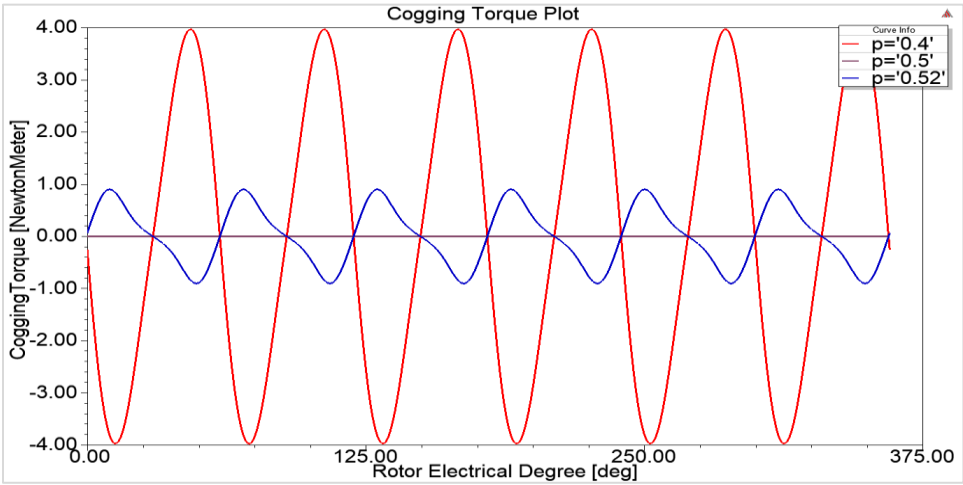

Figure 10 Variation of cogging torque versus rotor angle in degree

The comparison of performance parameters for various values of embrace factor is shown in *Table 5*. For the propulsion of EV at low speed, initially high rated torque is required with enough air gap density. As evident in *Table 4* the value of airgap flux density is highest at 0.4 value of embrace factor with less loss. But at some point, the effect of cogging torque is high. The lowest value occurred at 0.6 embrace factor with maximum losses. With less value of cogging torque and compromising the efficiency of motor the optimum intermediate value selected is 0.5 for air gap flux density and average value current. At this value the change in air gap density does not lead to extreme change in winding average current value. Permanent magnet may get demagnetized with abrupt and extreme variations of current and therefore due attention must be given on this parameter. No significant changes in average input current have been noticed while varying the pole embrace factor from 0.4 to 0.6. Most optimum values have been observed at pole embrace factor of 0.5, keeping the requirements of BEV.

The air gap flux density, average current and rated torque is determined parametrically with variation of the pole embrace factor presented in *Figure 11*.

Table 5 Comparison of performance parameters of BLDC motor at various pole embrace factor

p	Cogging torque (Nm)	Rated torque (Nm)	Efficiency (%)	AirGap flux density (T)	Average input current (A)	Total losses (W)
0.4	3.967	14.03	92.37	0.713	25.26	289.09
0.42	3.470	14.17	92.32	0.694	25.27	290.883
0.44	2.809	14.29	92.27	0.676	25.28	292.849
0.46	1.97	14.40	92.22	0.659	25.30	294.917
0.48	1.003	14.49	92.17	0.642	25.31	297.083
0.5	0.005	14.56	92.12	0.627	25.33	299.332
0.52	0.9009	14.61	92.06	0.612	25.34	301.669
0.54	1.613	14.63	92.00	0.598	25.36	304.104
0.56	2.091	14.63	91.94	0.5853	25.37	306.621
0.58	2.345	14.62	91.88	0.5727	25.39	309.219
0.6	2.432	14.59	91.81	0.5607	25.41	311.896

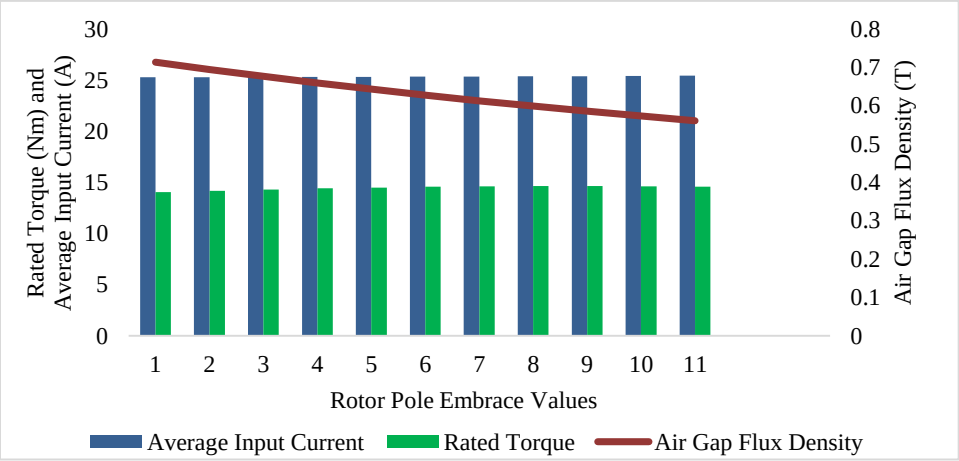

Figure 11 Graphical representation of air gap flux density, average current and rated torque with rotor pole embrace factor

5.Discussion

In this section the results pertaining to magnetic field parameters of BLDC motor using finite element technique have been discussed.

5.1FEM based analysis of BLDC motor

After performing an electrical analysis, ANSYS Maxwell is used to generate a FEM motor model using the periodic boundary condition of the inner magnetic field distribution of the motor. The ideal embrace value for the finite element-based model is

0.5. Transient analysis at rated load and rated speed is applied to a discrete time simulation that has been tuned for a time step of 2ms and a range of 0 to 60 ms. It generates the magnetic field distribution profile at a specific instant in time and rotor position. The structural design of the motor with mesh plot for full fraction model is shown in *Figure 12*. The distribution of magnetic field density of the motor is shown in the *Figure 13* and the magnetic forces acting on the surfaces/edges of the motor is shown in *Figure 14*. This elucidates that no saturation occurs in the motor and the maximum density of the magnetic flux exists in the stator tooth tip.

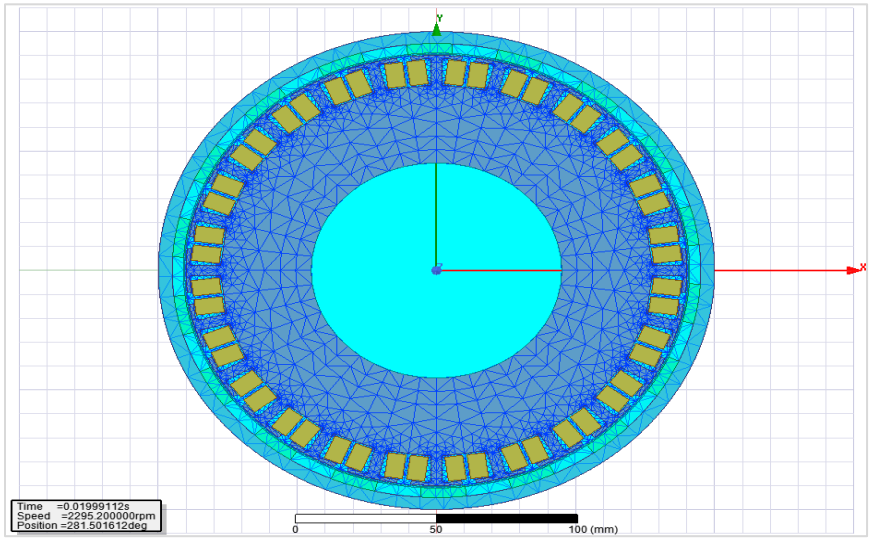

Figure 12 Mesh refinement of the motor

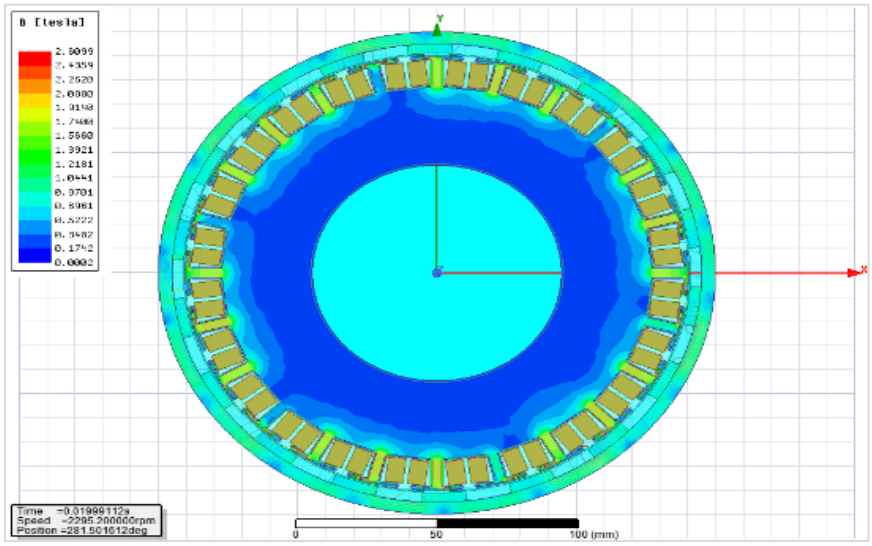

Figure 13 No load magnetic flux density distribution

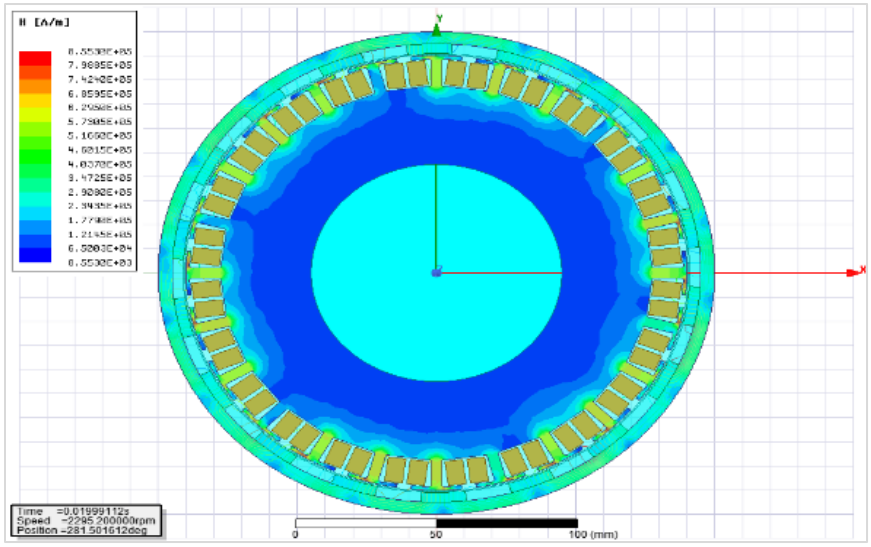

Figure 14 Vector potential of the motor

For the optimum design, the graph for electromagnetic torque is shown in *Figure 15*. The maximum peak value is 57.87 Nm and minimum is -5.06 Nm respectively. The average torque value is 50.16 Nm. The value of the ripple torque is 1.25 Nm. The ripple contents of the motor at this value are less in comparison to other values which enhance the life span of motor with less requirement of maintenance. The efficiency of the motor has improved by 1.15% compared to earlier reported design [24].

The variations in pole embrace factors of rotor led to the variation in unaligned position air gaps and thus providing more flux linkage at aligned position. The phase winding flux linkage and current for rated speed with time is shown in *Figure 16* and *Figure 17* respectively. The customized BEV has been designed as per the specifications shown in *Table 1*, keeping in view an optimum balancing between power, torque, and speed for IDC. Further the degree of freedoms in the finite element mesh have been optimized to properly analyses the magnetic field patterns inside the motor. Introduction of h-adaptivity refinement strategy has helped to reduce errors and improve the optimized design in comparison to similar kind of analysis as reflected in the literature survey.

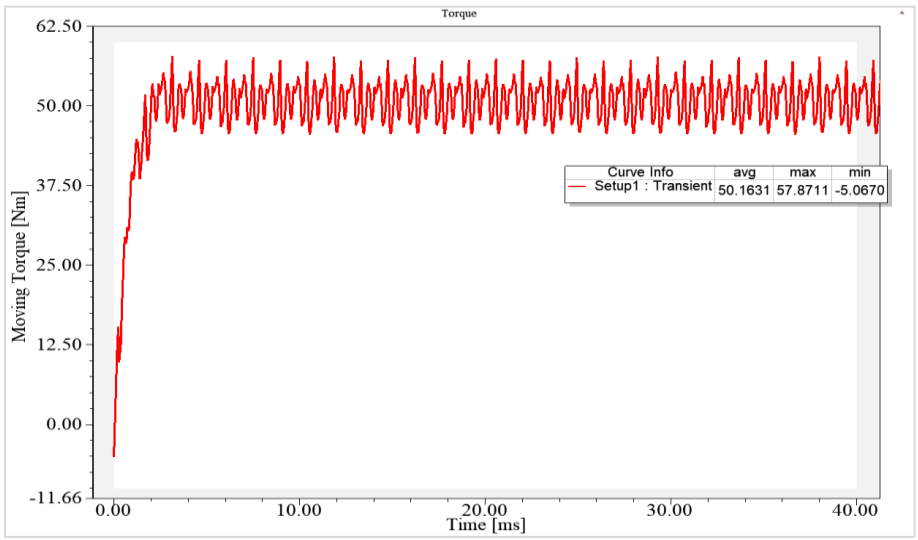

Figure 15 Plot showing variation torque and time at specific speed

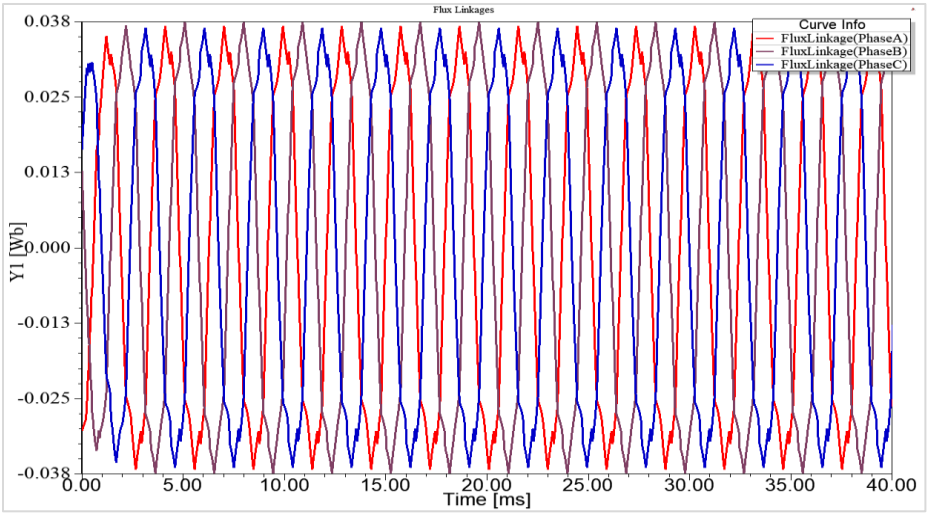

Figure 16 Winding flux linkage at rated speed

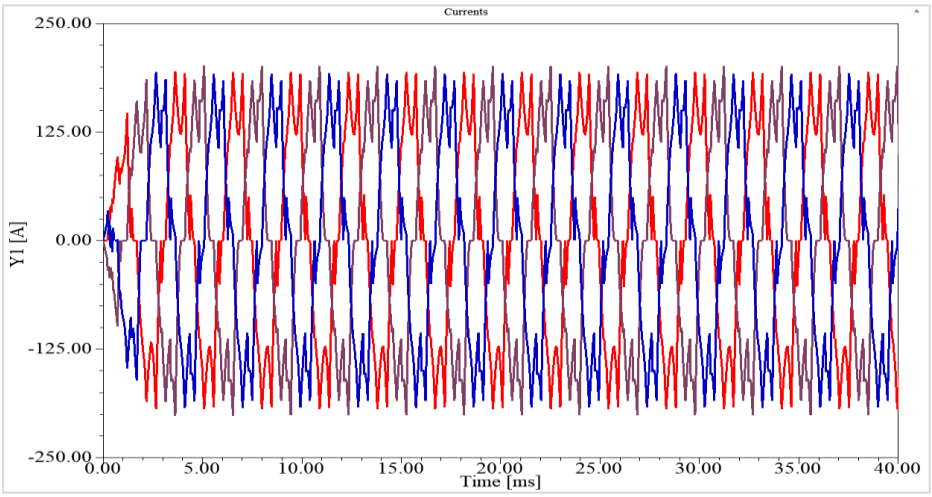

Figure 17 Winding current for rated speed

5.2Limitations

In this paper the customized design of the motor has been considered and as such it cannot be used for generalized sizing of the motor. Moreover h-adaptivity refinement strategy has been used to minimize the errors. However, an attempt may be made to minimize errors using p-adaptivity as well as hp adaptivity strategies. Further this paper projects the electromagnetic field studies of the motor and does not address the control strategies. Moreover, no hardware set-up has been established to carry the experimentation work and verify the results. Verification of results is based upon the simulation work carried by the other researchers.

The complete list of abbreviations is shown in *Appendix I.*

6.Conclusion and future work

The work presented illustrates how the rotor pole embrace factor affects a motor's performance in BEV. The parameter matching with BLDC motor has been determined using a kinematic equation. To determine an appropriate embrace factor with the minimum ripples and highest efficiency, parametric approach has been used. Based on the optimal value of the pole embrace factor, electromagnetic field analysis using finite elements is carried out. The smaller improvement of efficiency has a good impact on the state of health of the battery, which is powering the vehicle. In the proposed design of motor, the reduction in cogging torque plays a vital part in ensuring the vehicle's overall performance and for smooth driving pattern. The battery pack capacity requirement to propel the designed motor has been

computed. The electromagnetic torque generated by motor with this battery pack is enough to propel the vehicle. Therefore, a decrease in torque ripple decreases the motor's acoustic noise and vibrations, which in turn minimises the motor's eccentricity disbalancing issue and lengthens the battery electric vehicle's lifespan.

Acknowledgment
None.

Conflicts of interest
The authors have no conflicts of interest to declare.

Author's contributions statement
Rupam: Conceptualization, investigation on challenges, data analysis, data acquisition and writing the original draft. **Sanjay Marwaha:** Interpretation of results, review, supervision, reading proof and the revision of the whole article. **Anupma Marwaha:** Implementation of h-adaptive FEA for reduction of errors in optimized model.

References
[1] https://www.iea.org/reports/global-ev-outlook-2020. Accessed 10 June 2020.
[2] Chan CC. The state of the art of electric, hybrid, and fuel cell vehicles. Proceedings of the IEEE. 2007; 95(4):704-18.
[3] Barkenbus JN. Prospects for electric vehicles. Sustainability. 2020; 12(14):1-13.
[4] Jhunjhunwala A, Kaur P, Mutagekar S. Electric vehicles in India: a novel approach to scale electrification. IEEE Electrification Magazine. 2018; 6(4):40-7.
[5] Karki A, Phuyal S, Tuladhar D, Basnet S, Shrestha BP. Status of pure electric vehicle power train technology and future prospects. Applied System Innovation. 2020; 3(3):1-28.
[6] Dalal A, Kumar P. Design, prototyping, and testing of a dual-rotor motor for electric vehicle application. IEEE Transactions on Industrial Electronics. 2018; 65(9):7185-92.
[7] Chen Q, Xiao Q, Liao C, Zeng L, Li X, Huang J, et al. Design and analysis of outer rotor in-wheel motor for micro-electric vehicle. Advances in Mechanical Engineering. 2017; 9(11).
[8] Saidur R. A review on electrical motors energy use and energy savings. Renewable and Sustainable Energy Reviews. 2010; 14(3):877-98.
[9] Sandeep V, Shastri S. Analysis and design of PMBLDC motor for three wheeler electric vehicle application. In E3S web of conferences 2019 (pp. 1-7). EDP Sciences.
[10] Sun X, Shi Z, Lei G, Guo Y, Zhu J. Analysis and design optimization of a permanent magnet synchronous motor for a campus patrol electric vehicle. IEEE Transactions on Vehicular Technology. 2019; 68(11):10535-44.
[11] Yang Z, Shang F, Brown IP, Krishnamurthy M. Comparative study of interior permanent magnet, induction, and switched reluctance motor drives for EV and HEV applications. IEEE Transactions on Transportation Electrification. 2015; 1(3):245-54.
[12] Jain S, Kumar L. Fundamentals of power electronics controlled electric propulsion. Power Electronics Handbook. 2018:1023-65. Butterworth-Heinemann.
[13] Un-noor F, Padmanaban S, Mihet-popa L, Mollah MN, Hossain E. A comprehensive study of key electric vehicle (EV) components, technologies, challenges, impacts, and future direction of development. Energies. 2017; 10(8):1-84.
[14] Singh B, Singh S. State of the art on permanent magnet brushless DC motor drives. Journal of Power Electronics. 2009; 9(1):1-17.
[15] Jiang C, Qiao M, Zhu P, Zheng Q. Design and verification of high speed permanent magnet synchronous motor for electric car. In IEEE advanced information management, communicates, electronic and automation control conference 2018 (pp. 2371-5). IEEE.
[16] Jang SM, Jeong SS, Ryu DW, Choi SK. Design and analysis of high speed slotless PM machine with Halbach array. IEEE Transactions on Magnetics. 2001; 37(4):2827-30.
[17] Singh B, Singh BP, Dwivedi S. A state of art on different configurations of permanent magnet brushless machines. Journal-Institution of Engineers India Part El Electrical Engineering Division. 2006.
[18] Jokinen T, Hrabovcova V, Pyrhonen J. Design of rotating electrical machines. John Wiley & Sons; 2013.
[19] Toker K, Tosun O, Serteller NF, Topuz V. Design, optimization and experimental study of axial and hub BLDC motors in-wheel application for light electric vehicles. In IEEE Mediterranean electrotechnical conference 2022 (pp. 354-9). IEEE.
[20] Cabuk AS, Sağlam Ş, Üstün Ö. Impact of various slot-pole combinations on an in-wheel BLDC motor performance. IU-Journal of Electrical & Electronics Engineering. 2017; 17(2):3369-75.
[21] Thenmozhi G, Radhika A, Mithun B, Dhineesh M, Abissek B. A simulation-based investigation on the performance of BLDC motor used in electric vehicles for varied magnetic materials. In international conference on advanced computing and communication systems 2022 (pp. 875-9). IEEE.
[22] Guo L, Wang H. Research on stator slot and rotor pole combination and pole arc coefficient in a surface-mounted permanent magnet machine by the finite element method. World Electric Vehicle Journal. 2021; 12(1):1-15.
[23] Vadde A, Sachin S. Influence of rotor design in BLDC motor for two-wheeler electric vehicle. In 1st international conference on power electronics and energy 2021 (pp. 1-6). IEEE.
[24] Minh DB, Quoc VD, Huy PN. Efficiency improvement of permanent magnet BLDC motors for

electric vehicles. Engineering, Technology & Applied Science Research. 2021; 11(5):7615-8.
[25] Khalid MA, Othman RN, Zuki NA, Shukor FA, Othman MN, Chockalingam AV. Performance analysis of brushless DC motor with optimum magnetic energy for bicycle application. International Journal of Power Electronics and Drive Systems. 2021; 12(4):2113-22.
[26] Kumar A, Gandhi R, Wilson R, Roy R. Analysis of permanent magnet BLDC motor design with different slot type. In international conference on power electronics, smart grid and renewable energy 2020 (pp. 1-6). IEEE.
[27] Du G, Xu W, Zhu J, Huang N. Effects of design parameters on the multiphysics performance of high-speed permanent magnet machines. IEEE Transactions on Industrial Electronics. 2019; 67(5):3472-83.
[28] Li Y, Qu B, Zhu Y, Wan Y, Zhu X. Design and analysis of an outer rotor flux switching permanent magnet machine for light electric vehicles. International Journal of Applied Electromagnetics and Mechanics. 2019; 62(1):161-72.
[29] Yuan Y, Meng W, Sun X, Zhang L. Design optimization and analysis of an outer-rotor direct-drive permanent-magnet motor for medium-speed electric vehicle. World Electric Vehicle Journal. 2019; 10(2):1-19.
[30] He C, Wu T. Analysis and design of surface permanent magnet synchronous motor and generator. CES Transactions on Electrical Machines and Systems. 2019; 3(1):94-100.
[31] Mithunraj MK, Warrier GS, Pathivil P, Kanagalakshmi S, Archana R. Design and performance analysis of brushless DC motor using ANSYS maxwell. In 2nd international conference on intelligent computing, instrumentation and control technologies 2019 (pp. 1049-53). IEEE.
[32] Leitner S, Gruebler H, Muetze A. Cogging torque minimization and performance of the sub-fractional HP BLDC claw-pole motor. IEEE Transactions on Industry Applications. 2019; 55(5):4653-64.
[33] Popescu M, Goss J, Staton DA, Hawkins D, Chong YC, Boglietti A. Electrical vehicles-practical solutions for power traction motor systems. IEEE Transactions on Industry Applications. 2018; 54(3):2751-62.
[34] Patel AN, Suthar BN. Design optimization of axial flux surface mounted permanent magnet brushless dc motor for electrical vehicle based on genetic algorithm. International Journal of Engineering. 2018; 31(7):1050-6.
[35] Yildirim M, Kurum H, Miljavec D, Corovic S. Influence of material and geometrical properties of permanent magnets on cogging torque of BLDC. Engineering, Technology & Applied Science Research. 2018; 8(2):2656-62.
[36] He C, Wu T. Permanent magnet brushless DC motor and mechanical structure design for the electric impact wrench system. Energies. 2018; 11(6):1-24.
[37] Saed N, Mirsalim M. Mathematical modeling and analysis of dual-stator permanent magnet brushless DC motor. In annual power electronics, drives systems and technologies conference 2018 (pp. 48-52). IEEE.
[38] Sumithra P, Thiripurasundari D. Review on computational electromagnetics. Advanced Electromagnetics. 2017; 6(1):42-55.
[39] Sykulski J. Computational electromagnetics for design optimisation: the state of the art and conjectures for the future. Bulletin of the Polish Academy of Sciences: Technical Sciences. 2009; 57(2).
[40] Kumar A, Marwaha S, Singh A, Marwaha A. Comparative leakage field analysis of electromagnetic devices using finite element and fuzzy methods. Expert Systems with Applications. 2010; 37(5):3827-34.
[41] Dai M, Keyhani A, Sebastian T. Torque ripple analysis of a PM brushless DC motor using finite element method. IEEE Transactions on Energy Conversion. 2004; 19(1):40-5.
[42] Xie Q, Mu C, Wu G, Yu Z, Yu Y, Jia R. Method for flux linkage optimization of permanent magnet synchronous motor based on nonlinear dynamic analysis. Nonlinear Dynamics. 2019; 97(4):2067-89.
[43] Sadiku MN. Numerical techniques in electromagnetics. CRC Press; 2000.
[44] Zienkiewicz OC, Taylor RL, Zhu JZ. The finite element method: its basis and fundamentals. Elsevier; 2005.
[45] Chan CC, Chau KT. Design of electrical machines by the finite element method using distributed computing. Computers in Industry. 1991; 17(4):367-74.
[46] Yong JY, Ramachandaramurthy VK, Tan KM, Mithulananthan N. A review on the state-of-the-art technologies of electric vehicle, its impacts and prospects. Renewable and Sustainable Energy Reviews. 2015; 49:365-85.
[47] Grunditz EA, Thiringer T. Performance analysis of current BEVs based on a comprehensive review of specifications. IEEE Transactions on Transportation Electrification. 2016; 2(3):270-89.
[48] Sidharthan PV, Kashyap Y. Brushless DC hub motor drive control for electric vehicle applications. In first international conference on power, control and computing technologies 2020 (pp. 448-53). IEEE.
[49] Bhosale R, Warshe W, Shreelakshmi MP, Arlikar P, Prakash AK, Agarwal V. Performance comparison of two PWM techniques applied to BLDC motor control. In international conference on power, instrumentation, control and computing 2018 (pp. 1-6). IEEE.
[50] Ehsani M, Gao Y, Longo S, Ebrahimi KM. Modern electric, hybrid electric, and fuel cell vehicles. CRC Press; 2018.
[51] Larminie J, Lowry J. Electric vehicle technology explained. John Wiley & Sons; 2012.
[52] Ruoho S, Kolehmainen J, Ikaheimo J, Arkkio A. Interdependence of demagnetization, loading, and temperature rise in a permanent-magnet synchronous motor. IEEE Transactions on Magnetics. 2009; 46(3):949-53.
[53] Miller TJ. Brushless permanent-magnet and reluctance motor drives. 1989.

[54] Mellah H, Hemsas K. Simulations analysis with comparative study of a PMSG performances for small WT application by FEM. International Journal of Energy Engineering. 2013:55-64.
[55] Trout SR. Material selection of permanent magnets, considering thermal properties correctly. In proceedings: electrical insulation conference and electrical manufacturing and coil winding conference (Cat. No. 01CH37264) 2001 (pp. 365-70). IEEE.
[56] Krishnan R. Permanent magnet synchronous and brushless DC motor drives. CRC Press; 2017.
[57] Hanselman DC. Brushless permanent magnet motor design. The Writers' Collective; 2003.
[58] Marwaha S. Mitigation of cogging torque for the optimal design of BLDC motor. In 2nd international conference on electrical power and energy systems 2021 (pp. 1-5). IEEE.

Rupam received her B.Tech degree in Electrical Engineering in 2014 from Punjab Technical University, Jalandhar, India and M.Tech degree in Power Engineering in 2016 from Guru Nanak Dev Engineering College, Ludhiana, India. Currently, she is currently pursuing Ph.D. degree in Electrical and Instrumentation Engineering Department, SLIET, Longowal, Punjab, India. Her current research area of interest is Machine Design, Electric Vehicles Application, and Renewable Sources**.**
Email: rupamb92@gmail.com

Dr. Sanjay Marwaha received the Bachelor of Engineering (Electrical) degree from Gorakhpur University, Gorakhpur, India, in 1988, the Master of Engineering (Power System) from Punjab University, Chandigarh, India, in 1990, and the Ph.D. degree from Guru Nanak Dev University, Amritsar, India, in 2000. He is working as professor in the Department of Electrical and Instrumentation Engineering at Sant Longowal Institute of Engineering and Technology, Longowal, India since year 2002. His areas of interest include Design and Analysis of Electromagnetic Devices, Electrical and Electronic Measurement and Instrumentations, Electrical Machines, Power Systems, and High Voltage Engineering. He is having 175 research papers in his credit, which have been published in International and National journal as well as International and National conference proceedings of repute.
Email: marwaha_sanjay@yahoo.co.in

Dr. Anupma Marwaha did her BE in Electronics and Communication Engineering from PEC Chandigarh in 1990, M.Tech from REC Kurukshetra in 1992. and Ph. D. Degree from Guru Nanak Dev University, Amritsar in the year 2003. She started her teaching career as Lecturer at NIT (earlier REC) Kurukshetra and has total teaching experience of thirty years. She has worked at various key positions at reputed Institutions including SLIET Longowal, BCET Gurdaspur and NIT kurukshetra. She has supervised 21 M.Tech candidates, 15 Ph.D candidates and 03 Ph.D candidates are in progress. She has 104 research publications to her credit in National and International Journals of repute and 85 research papers published in various National and International Conferences.
Email: marwaha_anupma@yahoo.co.in

Appendix I

S. No.	Abbreviation	Description
1	AFSPMBLDC	Axial Flux Surface-Mounted Permanent Magnet Type Brushless DC Motor
2	Alnicos	Aluminum, Nickel, Cobalt, and Iron
3	BEV	Battery Electric Vehicle
4	BLDC	Brushless Direct Current
5	CCC	Current Chopped Control
6	DC	Direct Current
7	EMF	Electro-Motive Force
8	EPC	Electronic Power Control
9	EV	Electric Vehicle
10	FEA	Finite Element Analysis
11	FEM	Finite Element Method
12	GA	Genetic Algorithm
13	GHG	Green House Gas
14	PMBLDC	Permanent Magnet Brushless Direct Current
15	IDC	Indian Driving Cycle
16	IM	Induction Motor
17	IPMBLDCM	Internal Permanent Magnet Brushless DC Motor
18	Li-Ion	Lithium-Ion
19	LMV	Light Motor Vehicles
20	NdFeB	Neodymium Iron and Boron
21	PMSM	Permanent Magnet Synchronous Motor
22	SRM	Switched Reluctance Motor
23	ZEVs	Zero Emission Vehicles